

AD-A001 275

UNCLASSIFIED

File Library
NSWC

USADAC TECHNICAL LIBRARY



5 0712 01019314 1

DTIC

8
K14 Jmm

Technical Report

distributed by



Defense Technical Information Center
DEFENSE LOGISTICS AGENCY

Cameron Station • Alexandria, Virginia 22304-6145

UNCLASSIFIED

NOTICE

We are pleased to supply this document in response to your request.

The acquisition of technical reports, notes, memorandums, etc., is an active, ongoing program at the Defense Technical Information Center (DTIC) that depends, in part, on the efforts and interests of users and contributors.

Therefore, if you know of the existence of any significant reports, etc., that are not in the DTIC collection, we would appreciate receiving copies or information related to their sources and availability.

The appropriate regulations are Department of Defense Directive 3200.12, DoD Scientific and Technical Information Program; Department of Defense Directive 5200.20, Distribution Statements on Technical Documents (amended by Secretary of Defense Memorandum, 18 Oct 1983, subject: Control of Unclassified Technology with Military Application); Military Standard (MIL-STD) 847-B, Format Requirements for Scientific and Technical Reports Prepared by or for the Department of Defense; Department of Defense 5200.1R, Information Security Program Regulation.

Our Acquisition Section, DTIC-FDAB, will assist in resolving any questions you may have. Telephone numbers of that office are: (202)274-6847, 274-6874 or Autovon 284-6847, 284-6874.

FEBRUARY 1984

★U.S. Government Printing Office: 1986-491-133/43651

AD/A-001 275

SCALING OF MUZZLE BRAKE PERFORMANCE
AND BLAST FIELD

L. L. Pater

Naval Weapons Laboratory
Dahlgren, Virginia

October 1974

DISTRIBUTED BY:

NTIS

National Technical Information Service
U. S. DEPARTMENT OF COMMERCE

UNCLASSIFIED

SECURITY CLASSIFICATION OF THIS PAGE (When Data Entered)

AD/A 001 275

REPORT DOCUMENTATION PAGE		READ INSTRUCTIONS BEFORE COMPLETING FORM
1. REPORT NUMBER TR-3049	2. GOVT ACCESSION NO.	3. RECIPIENT'S CATALOG NUMBER
4. TITLE (and Subtitle) SCALING OF MUZZLE BRAKE PERFORMANCE AND BLAST FIELD		5. TYPE OF REPORT & PERIOD COVERED
7. AUTHOR(s) L. L. Pater, Ph.D		6. PERFORMING ORG. REPORT NUMBER
9. PERFORMING ORGANIZATION NAME AND ADDRESS Naval Surface Weapons Center Dahlgren Laboratory Dahlgren, Va. 22448		8. CONTRACT OR GRANT NUMBER(s)
11. CONTROLLING OFFICE NAME AND ADDRESS		10. PROGRAM ELEMENT, PROJECT, TASK AREA & WORK UNIT NUMBERS
12. REPORT DATE October 1974		13. NUMBER OF PAGES
14. MONITORING AGENCY NAME & ADDRESS (if different from Controlling Office)		15. SECURITY CLASS. (of this report) UNCLASSIFIED
16. DISTRIBUTION STATEMENT (of this Report) Approved for public release; distribution unlimited		15a. DECLASSIFICATION/DOWNGRADING SCHEDULE
17. DISTRIBUTION STATEMENT (of the abstract entered in Block 20, if different from Report)		
18. SUPPLEMENTARY NOTES		
19. KEY WORDS (Continue on reverse side if necessary and identify by block number) Reproduced by NATIONAL TECHNICAL INFORMATION SERVICE U.S. Department of Commerce Springfield VA 22151		
20. ABSTRACT (Continue on reverse side if necessary and identify by block number) Experimental muzzle brake performance tests were carried out at reduced scale, using a 40mm free-recoil gun apparatus, for comparison with available 105mm data. Results were sufficient to conclude that muzzle devices can be accurately investigated and developed at reduced scale, with considerable savings of time and money. The apparatus and procedures developed are, with minor modifications, satisfactory for carrying out reduced scale testing. (S)		

DD FORM 1 JAN 73 1473

EDITION OF 1 NOV 68 IS OBSOLETE
S. R. 0102-010-0001

UNCLASSIFIED

SECURITY CLASSIFICATION OF THIS PAGE (When Data Entered)

NWL TECHNICAL REPORT TR-3049
October 1974

SCALING OF MUZZLE BRAKE
PERFORMANCE AND BLAST FIELD

by

L. L. Pater, Ph.D
Test and Evaluation Department

Approved for public release; distribution unlimited.

NAVAL SURFACE WEAPONS CENTER
DAHLGREN LABORATORY
Dahlgren, Virginia



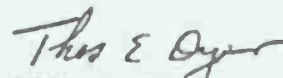
ia

FOREWORD

This report was prepared as part of the development program for a muzzle brake to be used in connection with a Naval Ordnance Systems Command Exploratory Development Program; Large Caliber (203mm) Lightweight Field Artillery Weapon. In addition, the program aims to advance the state-of-the-art of muzzle brake design procedures. The work was carried out under ORD Task No. 35C/501/090/1UF32353/517, a NOSC program sponsored by the Marine Corps Education and Development Command.

This report has been reviewed and approved by J. J. Yagla and R. Shank of the Special Projects Division.

Released by:



THOS. E. DYER, Head
Test and Evaluation Department

ABSTRACT

Experimental muzzle brake performance tests were carried out at reduced scale, using a 40mm free-recoil gun apparatus, for comparison with available 105mm data. Results were sufficient to conclude that muzzle devices can be accurately investigated and developed at reduced scale, with considerable savings of time and money. The apparatus and procedures developed are, with minor modifications, satisfactory for carrying out reduced scale testing.

CONTENTS

	<u>Page</u>
FOREWORD	i
ABSTRACT	11
LIST OF FIGURES	1v
LIST OF TABLES	1v
NOMENCLATURE	v
INTRODUCTION	1
THEORETICAL SCALING CONSIDERATIONS	6
EXPERIMENTAL APPARATUS AND PROCEDURES	13
RESULTS AND DISCUSSION	27
REFERENCES	36
APPENDIXES:	
A. REDUCED DATA	
B. EXPERIMENTAL UNCERTAINTY ANALYSIS	
C. DISTRIBUTION	

LIST OF FIGURES

	<u>Page</u>
1. Schematic of Muzzle Brake	3
2. Schematic of 40mm Free-Recoil Gun Mount	15
3. 40mm Free-Recoil Gun Mount	16
4. Round Configuration, 40mm Scaling 105mm	18
5. Instrumentation Schematic	19
6. Typical Raw Data Record	24
7. Representative Displacement, Velocity, and Acceleration of Recoiling Mass in Free Recoil	26
8. Comparison of Muzzle Brake Effectiveness Data	29
9. Comparison of Blast Overpressure with Muzzle Brake; Gage Location 142°, 28.4 Calibers	32

LIST OF TABLES

1. Significant Parameters for Scaling of Gun and Muzzle Brake Performance	8
2. Similarity Parameters	11
3. Model Law for Scaling Gun Performance, Including Muzzle Brake	12
4. Scaled Parameter Values	21
5. Scaled Charge Determination Test	22
6. Comparison of Muzzle Brake Effectiveness Data	28
7. 105mm Blast Data	30
8. Comparison of Blast Overpressure Results Without Muzzle Brake	31
A-1. Masses of Apparatus	A-1
A-2. Experimental Data	A-2
A-3. Experimental Data	A-3
A-4. Experimental Data	A-4
A-5. Experimental Data	A-5
A-6. Experimental Data	A-6
A-7. Reduced Experimental Data for Muzzle Brake Effectiveness	A-7

NOMENCLATURE

A	bore area
a_o	speed of sound in atmosphere
c	caliber of gun (bore diameter at lands)
D	propellant grain diameter
d	propellant grain perforation diameter
E	muzzle brake efficiency
E_y	Young's modulus of muzzle brake material
F_B	force exerted on muzzle brake
G	gas-ejection impulse
H	height of point of interest in blast field
h	muzzle height
I	recoil impulse
I_B	impulse on muzzle brake by propellant gas
I_p	pressure impulse
L	travel distance
l	in-bore shot travel
l_c	propellant grain length
l_i	dimensions of objects in blast field
l_j	muzzle brake linear dimension:
M	in-bore portion of recoil impulse
m_c	mass of propellant
m_p	mass of projectile
m_{rl}	recoiling mass with muzzle brake

NOMENCLATURE (Continued)

m_{r2}	recoiling mass without muzzle brake
m_r	recoiling mass (with or without muzzle brake)
N	number of perforations in propellant grain
P_B	pressure on muzzle brake
P_E	engraving pressure
P_m	muzzle pressure
P_{max}	peak overpressure
P_o	atmospheric pressure
RT_o	specific impetus of propellant
T	duration of blast wave
T_f	flame temperature
t	elapsed time
U_c	chamber volume
V_p	projectile ejection velocity (muzzle velocity)
V_{r1}	terminal recoil velocity with muzzle brake
V_{r2}	terminal recoil velocity without muzzle brake
V_{rp}	recoil velocity at instant of projectile ejection
V_{rt}	terminal recoil velocity (with or without muzzle brake)
x	distance along line of fire
y	distance from axis of fire
α	barrel angle (Q.E.)
β	muzzle brake effectiveness
γ_c	ratio of specific heats of propellant gas

SYMBOLIC INCLOSURE (Continued)

γ_0	ratio of specific heats of atmosphere
ϵ	strain
λ	model/projectile caliber ratio
ρ_B	density of case brake material
ρ_C	propellant density
σ	stress
τ	arrival time of blast wave

INTRODUCTION

BACKGROUND

The Armed Forces are currently engaged in the development of lightweight artillery for increased mobility. Such lightweight guns must utilize every available means to reduce the maximum recoil force transmitted to the gun carriage. Reduction of the transmitted recoil force is necessary to prevent displacement of the lightweight gun carriage during firing.

When a gun is fired, the burning propellant produces high temperature, high pressure gas. This high pressure gas accelerates the projectile forward and also exerts a rearward force on the recoiling mass. The time integral of the recoil force is called the "recoil impulse," denoted by I . Most of the recoil impulse (typically 70 to 90%) occurs while the projectile is in the gun barrel. This portion of the recoil impulse is called the "in-bore impulse," denoted by M . However, after the projectile has been ejected, the barrel still contains high pressure gas. The "gas-ejection period" is defined as the time from projectile ejection to the time when conditions in the barrel reach equilibrium with the environment. During the gas-ejection period, as the propellant gas flows out of the barrel, the gun closely resembles a rocket. The impulse exerted on the recoiling parts during the gas-ejection period is referred to as the "gas-ejection impulse," denoted by G , and constitutes the remainder of the recoil impulse exerted on the gun by the propellant gas. Thus,

$$I = M + G \quad (1)$$

for a gun without a muzzle device.

The recoil impulse consists of a recoil force which is typically very large but is of quite short duration.* For closed breech weapons, artillery weapon designers employ a hydraulic-pneumatic recoil system to spread the response to the recoil impulse over a longer time span, thus reducing the maximum force exerted on the carriage. The particular recoil system variant known as the "soft recoil" or "firing out of battery" system simply uses the same principle to achieve an even longer time span and hence further reduce the force on the carriage, without requiring excessive recoil length. Another method of reducing the maximum force on the carriage is to reduce the recoil impulse.

*For example, the peak recoil force in a 5"/54 Naval gun is on the order of 1.1×10^6 lb, but drops to about 10% of this value within about 15 ms.

DESCRIPTION OF MUZZLE BRAKE

The net recoil impulse can be reduced through use of a "muzzle brake" on the muzzle of a gun. A simplified muzzle brake is shown in Figure 1, consisting essentially of a baffle mounted some distance in front of, and rigidly connected to, the gun muzzle, with a port in the baffle through which the projectile passes. As the propellant gas rushes out of the muzzle, a portion of the gas impinges on the baffle and is deflected from the axial direction. This deflection of high-speed gas from the axial direction by the muzzle brake results in a decrease in the axial momentum of the gas, and hence a forward impulse on the muzzle brake. The forward impulse exerted on the muzzle brake is denoted by I_B . Since the muzzle brake is attached to the barrel, the forward impulse is in turn exerted on the recoiling parts, thus reducing the net recoil impulse. The forward impulse can be increased by effecting a larger decrease in the axial momentum of the propellant gas. This can be achieved by deflecting more of the propellant gas, by turning the gas through a larger angle, and by causing the gas speed to increase as the gas is turned. It is possible, with a highly efficient muzzle brake on certain guns, that the forward impulse can amount to over 50% of the normal recoil impulse, so that the resultant recoil impulse would be less than half as large as that which would occur for the same gun without a muzzle brake.

A restriction on the use of muzzle brakes is that the blast overpressure is considerably increased in the region behind the muzzle, which includes the crew area. A more efficient muzzle brake (i.e., one which yields a larger forward impulse) usually results in a higher blast overpressure in the crew area. It is possible, however, to achieve significant reduction of recoil impulse and yet maintain an acceptable blast overpressure.

A possible disadvantage of the muzzle brake is that it has no effect until after the projectile has been ejected from the barrel, after most of the normal rearward recoil impulse has already occurred. Thus the action of the muzzle brake in reducing the net recoil impulse can be said to be "corrective" rather than "preventive." The muzzle brake can nevertheless be very advantageous, since the total recoil impulse which must be absorbed by the recoil mechanism can be considerably reduced.

MUZZLE BRAKE PERFORMANCE PARAMETERS

The two primary muzzle brake performance parameters are the blast overpressures and some sort of efficiency parameter. The blast overpressures are usually specified simply as peak overpressure levels and blast wave durations, at certain specified locations around the gun.

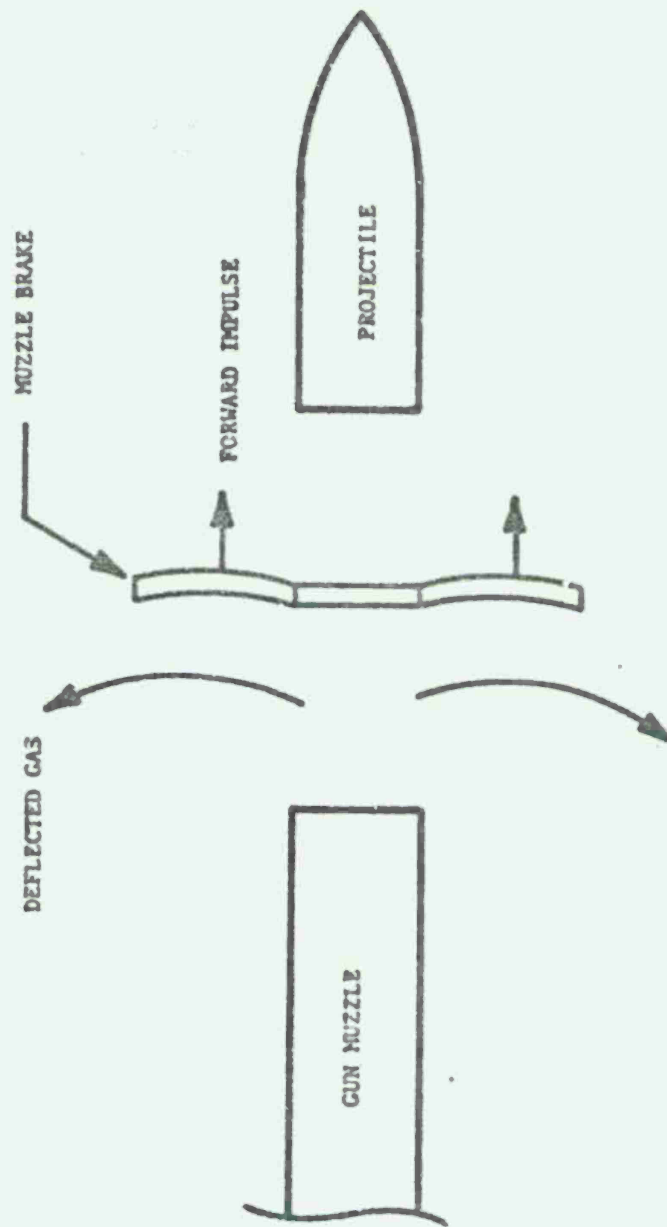


Figure 1. Schematic of Muzzle Brake

There is some difference of opinion concerning the best parameters for measuring muzzle brake efficiency. There are basically two efficiency parameters currently in use. The first, denoted by the symbol E, is defined as the ratio of the forward impulse due to the muzzle brake to the total recoil impulse without a muzzle brake,

$$E = \frac{I_B}{I} \quad (2)$$

This parameter can be accurately measured experimentally with relative ease. The value of I can be obtained by measuring the recoil impulse for shots without a muzzle brake. The value of I_B can be determined as the difference in recoil impulse for shots with and without the muzzle brake.

However, the parameter is not actually a measure of the performance of the muzzle brake design. Rather, it is a measure of the performance of the muzzle brake when used on a specific gun. The in-bore impulse M is essentially independent of the presence of a muzzle brake, since the muzzle brake is operative only during the gas-ejection period. Yet, the in-bore impulse M, and, likewise, the gas-ejection impulse G, can be a significantly different fraction of the total recoil impulse I for different gun designs. Thus, a given muzzle brake design could be tested on two guns which had the same value of I but different values of G, with the result that significantly different values of efficiency E could be obtained. The importance of this is that the parameter E cannot be easily used to compare and evaluate different muzzle brake designs unless prototypes of each brake have been tested on the same type of gun. In addition, there is no clear upper limit for the value of E against which the performance of a muzzle brake design can be compared. The conclusion of the writer is that the efficiency parameter E is not adequate for comparison and evaluation of muzzle brake designs.

The second muzzle brake performance parameter currently in use is denoted in this report by the symbol B and is called "muzzle brake effectiveness," also known as "momentum index" or "muzzle brake efficiency." It is defined as the ratio of the forward impulse due to the muzzle brake to the gas ejection impulse G without a muzzle brake,

$$B = \frac{I_B}{G} \quad (3)$$

This is a more meaningful measurement of muzzle brake performance since I_B is normalized by G, which is the impulse that the muzzle brake can affect. Experience indicates that the value of B is

relatively constant for a given brake design, even when the brake design is used on different guns or on the same gun with different propellant charges. Thus, the parameter β is quite useful for comparing performance of different muzzle brake designs.

The magnitude of the muzzle brake effectiveness, β , has some physical significance. If all of the gas were turned through an angle of exactly 90° , then I_B would be equal to C , and so the value of β would be 1 (equation 3). If all of the gas were turned through an angle of 180° , then $I_B = 2C$ and $\beta = 2$, which is the upper limiting value for β . Thus, $0 \leq \beta \leq 2$. This picture of the operation of a muzzle brake is admittedly oversimplified. For example, the possibility that the speed of the gas could change as the gas is turned is ignored. Nonetheless, at least limited physical significance can be attached to the value of β .

The primary disadvantage of the muzzle brake effectiveness parameter β is that the value of C is not easy to determine accurately.

DESIGN PROCEDURES

Designing a muzzle brake to yield a large forward impulse, yet an acceptable blast overpressure in the crew areas, and of a reasonable size, weight, and sufficient strength, is a formidable design problem. In the past, muzzle brakes have been developed largely by experimental trial-and-error on the full-sized gun for which they were being designed. Such design procedure is expensive in terms of both time and money. In addition, accurate muzzle brake performance data are very difficult to obtain on conventional gun mounts. The present work is a portion of a larger effort to provide a less expensive and more fruitful method of muzzle brake development.

This report describes a technique for accurate experimental testing of muzzle brake performance at reduced scale, which can greatly reduce the cost of muzzle brake development and testing. A further advantage is that a muzzle brake could be developed, at reduced scale, for a large gun that is in the "feasibility study" stage of its evolution.

A concurrent investigation, conducted by Dr. F. H. Maillie (1)* of the Naval Weapons Laboratory, is concerned with analytical prediction of muzzle brake performance. Such an analytical technique would be used to guide the design and optimization of muzzle brakes, with developmental testing carried out at reduced scale. Only limited full-

*Numbers in brackets refer to numbered references listed at the end of this report.

scale testing would be required for final verification of the performance of the brake design at full scale.

The analytical technique is currently limited to axisymmetric muzzle devices. For guns that must fire over earth, such as Army and Marine artillery, the bottom of the muzzle brake must be closed to avoid dust obscuration. The top of the muzzle brake must also be closed to prevent unbalanced forces normal to the gun barrel. Flow through such a muzzle device is highly three-dimensional; current computer hydrocodes are not suitable for analysis of such three-dimensional unsteady gas dynamic situations. Design of such a muzzle brake would have to be primarily empirical. However, the analytical technique can provide valuable guiding information even for such designs.

OBJECTIVE

The purpose of the present work is to investigate the feasibility of reduced scale testing of muzzle brake performance. Parameters of primary interest include muzzle brake effectiveness, recoil force-time history, the blast overpressure field, and strength of the brake and attachment hardware. In addition to reducing cost, using a small gun facilitates use of a "free-recoil" gun mount, which appears to be the best test vehicle for investigating muzzle brake performance.

A further objective is to develop a suitable free-recoil gun mount test apparatus and procedures for use in future muzzle brake development. The same apparatus could also be used to study at reduced scale other facets of gun performance.

THEORETICAL SCALING CONSIDERATIONS

The events of primary interest in muzzle brake investigation occur during the gas-ejection period, since this is when the muzzle brake is operative. It is desired to instrument and test a small gun equipped with a muzzle brake to predict the behavior of a much larger gun and muzzle brake. This requires that the gas flow during the gas-ejection period of the model gun be geometrically and dynamically "similar" (in the strict similitude sense) to the gas-ejection period gas flow of the prototype gun. Note that the requirement that the gas flow be geometrically similar requires the model gun barrel to be a scale replica of the prototype. Also, the requirement of dynamic similarity requires, as a necessary condition, that the initial conditions of the gas-ejection period must scale. These conditions are the final conditions of the in-bore period.

It appears that the most practicable method of achieving a scaled gas-ejection period is to also require a scaled in-bore period. Such an approach has the additional advantage that the apparatus can be used to study, at reduced scale, other phenomena which occur during the in-bore period as well as the gas-ejection period.

The approach used to achieve accurately scaled gun and muzzle brake performance is to scale in detail the interior ballistics of the prototype gun, based on a scaling analysis by Dr. J. East (2). The scaling analysis proceeds in the normal manner, in which a set of significant dimensional parameters is chosen and then combined into a set of dimensionless similarity parameters by means of the techniques of dimensional analysis (Buckingham π Theorem). The list of dimensional parameters considered to be significant is shown in Table 1, with one possible set of similarity parameters shown in Table 2.

For a correctly chosen set of dimensional parameters, maintaining the same value of each similarity parameter for model and prototype results in valid scaling. Consideration of the similarity parameters leads to a "model law," a detailed accounting of how each dimensional parameter must scale. The caliber ratio, denoted by λ , is defined as:

$$\lambda = \text{caliber ratio} = \frac{c_{\text{model}}}{c_{\text{prototype}}} \quad (4)$$

Geometric similarity (for instance, π groups 1 through 4) requires that all linear dimensions have the scale factor λ . Atmospheric conditions will be (at least nearly) the same for model and prototype, so P_0 , ρ_0 , and γ_0 must all have a scale factor of unity. This in turn requires that all pressures and velocities have a scale factor of unity, as can be seen by comparison of π groups 10, 15, 19, and 30 or 12 and 14. This is a realistic requirement, since most guns of interest regardless of size, have roughly the same projectile muzzle velocity. Since pressure has a scale factor of unity, π_{10} shows that force has a scale factor of λ^2 . Then π_{20} shows that density has a scale factor of unity. Further reasoning along the same lines leads to the model law shown in Table 3. Of particular interest is the fact that Young's modulus, density, stress, and strain of the muzzle brake material all have a scale factor of 1, so that the same material can be used for the muzzle brake model and prototype. Further, the strength of the muzzle brake can also be easily investigated experimentally at reduced scale.

The model law shown in Table 3 is quite detailed and may seem unwieldy, but is actually not difficult to use. It is, however, not usually possible to satisfy all requirements of the model law exactly. For example, the specific impetus (RT_0) of the propellant is one of the most important parameters for obtaining a given gun performance, but in practice its value varies for different propellant lots. To obtain accurately scaled gun performance, it may then be necessary to vary some other parameter such as chamber volume or mass of propellant. Another difficulty is that exact scale replica propellant grains are usually not available.

Table 1. Significant Parameters for Scaling of
Gun and Muzzle Brake Performance

<u>Symbol</u>	<u>Quantity</u>	<u>Fundamental Dimensions</u>
<u>Gun Geometry</u>		
x	distance along line of fire	length
y	distance from axis of fire	length
h	muzzle height	length
H	height of point of interest	length
α	barrel angle (Q.E.)	radians
l	in-bore shot travel	length
c	caliber of gun (bore diameter at lands)	length
l_i	dimensions of other obstructions	length
A	bore area	length ²
U_c	chamber volume	length ³
<u>Ambient Atmospheric Environment</u>		
P_o	atmospheric pressure	force/length ²
γ_o	ratio of specific heats of atmosphere	dimensionless
a_o	speed of sound in atmosphere	length/time
<u>Interior Ballistics</u>		
m_p	mass of projectile	force-time ² /length
V_p	projectile ejection velocity (muzzle velocity)	length/time
P_E	engraving pressure	force/length ²
t	elapsed time	time
m_c	mass of propellant	force-time ² /length

Table 1. Significant Parameters for Scaling of Gun and Muzzle Brake Performance (Continued)

<u>Symbol</u>	<u>Quantity</u>	<u>Fundamental Dimensions</u>
RT_o	specific impetus ("Force" of propellant)	$\text{length}^2/\text{time}^2$ (length-force/mass)
γ_c	ratio of specific heats of propellant gas	dimensionless
T_f	flame temperature	temperature
ρ_c	propellant density	$\text{force-time}^2/\text{length}^4$
D	propellant grain diameter	length
l_c	propellant grain length	length
N	number of perforations	dimensionless
d	propellant grain perforation diameter	length
<u>Blast Field</u>		
P_{\max}	peak overpressure	$\text{force}/\text{length}^2$
I_p	pressure impulse	$\text{force-time}/\text{length}^2$
τ	arrival time	time
T	duration of blast wave	time
P_m	muzzle pressure	$\text{force}/\text{length}^2$

Table 1. Significant Parameters for Scaling of Gun and Muzzle Brake Performance (Continued)

<u>Symbol</u>	<u>Quantity</u>	<u>Fundamental Dimensions</u>
	<u>Muzzle Brake</u>	
l_j	muzzle brake linear dimensions	length
p_B	pressure on muzzle brake	force/length ²
σ	stress	force/length ²
ϵ	strain	dimensionless
ρ_B	density of muzzle brake material	force-time ² /length ⁴
E_y	Young's modulus of muzzle brake	force/length ²
F_B	force exerted on muzzle brake	force
I	recoil impulse	force-time
M	in-bore impulse	force-time
G	gas-ejection impulse	force-time
I_g	impulse on muzzle brake by propellant gas	force-time
β	muzzle brake effectiveness	dimensionless

Table 2. Similarity Parameters

$\pi_1 = y/c$	$\pi_{21} = D/c$
$\pi_2 = x/c$	$\pi_{22} = l_c/c$
$\pi_3 = h/c$	$\pi_{23} = N$
$\pi_4 = H/c$	$\pi_{24} = d/c$
$\pi_5 = \alpha$	$\pi_{25} = P_{\max} c^2/F_B$
$\pi_6 = 1/c$	$\pi_{26} = I_p c^2/F_B$
$\pi_7 = l_1/c$	$\pi_{27} = \tau/T$
$\pi_8 = A/c^2$	$\pi_{28} = T/t$
$\pi_9 = U_c/c^3$	$\pi_{29} = l_j/c$
$\pi_{10} = P_o c^2/F_B$	$\pi_{30} = P_B c^2/F_H$
$\pi_{11} = \gamma_o$	$\pi_{31} = c^2/F_B$
$\pi_{12} = a_o t/c$	$\pi_{32} = c$
$\pi_{13} = \pi_p c/F_B t^2$	$\pi_{33} = \rho_B c^4/F_B t^2$
$\pi_{14} = V_p t/c$	$\pi_{34} = E_y c^2/F_B$
$\pi_{15} = P_E c^2/F_B$	$\pi_{35} = I/F_B t$
$\pi_{16} = m_c c/F_B t^2$	$\pi_{36} = M/F_B t$
$\pi_{17} = (RT_o) T^2/c^2$	$\pi_{37} = G/F_B t$
$\pi_{18} = \gamma_c$	$\pi_{38} = I_B/F_B t$
$\pi_{19} = T_f/T_f$	$\pi_{39} = B$
$\pi_{20} = \rho_C c^4/F_B t^2$	

Table 3. Model Law for Scaling Gm Performance,
Including Muzzle Brake

<u>Quantity</u>	<u>Fundamental Dimensions</u>	<u>Symbols</u>	<u>Scale Factor*</u>
Linear Dimensions	length	$y, x, h, H, l, c,$ D, l_c, d, l_j, l_i	λ
Area	length ²	A	λ^2
Volume	length ³	U_c	λ^3
Pressure	force/length ²	$P_o, P_{max}, P_E, P_B, P_m$	1
Sonic Velocity	length/time	a_o	1
Velocity	length/time	V_p	1
Mass	force-time ² /length	m_p, m_c	λ^3
Density	force-time ² /length ⁴	ρ_c, ρ_B	1
Time	time	T, τ, t	λ
Energy	force-length	E	λ^3
Temperature	temperature	T_f	1
Force	force	F_B	λ^2
Stress	force/length ²	σ	1
Strain	dimensionless	c	1
Young's modulus	force/length ²	E_y	1
Impulse	force-time	I, M, C, I_B	λ^3
Pressure Impulse	force-time/length ²	I_p	λ
Specific Impetus	length ² /time ²	RT_o	1
Dimensionless Parameters	dimensionless	γ_o, γ_c, B, N	1
Angles	radians	α	1

* $\lambda = \text{caliber ratio} = \frac{c_{\text{model}}}{c_{\text{prototype}}}$

Adjustment in parameter values may also have to be made to compensate for variations in parameters not included in the model law. Several parameters were not included because either they were considered to have a negligible effect, or they were extremely difficult to predict and control. Examples of such parameters include the effect of case crimping and rotating band engraving on shot-start pressure, friction effects, rotational kinetic energy of the projectile, gas leakage, variation in thermodynamic properties of the gas, and heat transfer effects. Experience has indicated that successful scaling can be achieved by minor adjustments in other parameters, at least if model and prototype are of basically similar design.

EXPERIMENTAL APPARATUS AND PROCEDURES

DESIGN OF EXPERIMENT

The scaling technique described must be verified before it can be used with confidence. Satisfactory verification could be made if accurate muzzle brake performance data for a large gun were available and could be reproduced at reduced scale using the model law.

Budget limitations did not allow the large gun experimental data to be obtained as part of the current program. However, apparently satisfactory data were available, from the research of Salisbury (3), for a 105mm Howitzer mounted in a free-recoil gun mount. Salisbury tested a number of muzzle brakes, consisting of flat circular disks of various diameters, mounted at various distances from the muzzle. Values of muzzle brake effectiveness and of blast overpressure at locations behind the muzzle are given for each brake configuration. The values of most parameters listed in the model law are available for the 105mm Howitzer used by Salisbury.

The verification of the scaling technique consisted of duplicating selected portions of Salisbury's 105mm experiments at reduced scale, using a 40mm free-recoil gun mount apparatus. Agreement of brake effectiveness β and blast overpressure results would provide verification of the scaling technique. The apparatus and technique could then be used with confidence in future muzzle brake design programs.

FREE-RECOIL GUN MOUNT TEST APPARATUS

The apparatus used in the muzzle brake scaling investigation is a "free-recoil" gun mount. The term "free-recoil" means that the recoiling parts are free to recoil with no retarding force present. This situation cannot actually be achieved because of the presence of friction, but can be approached by reducing friction as much as possible. The advantage of a free-recoil gun mount is that the motion of the gun can be easily related to the recoil forces acting on the gun.

The gun used in the free-recoil gun mount is a 40mm Naval saluting gun with a hand-operated sliding breech. The barrel is a MK 1 water-cooled barrel with the cooling jacket removed to reduce weight. The 40mm gun is particularly suitable as a model gun for a number of reasons, including that it is of basically similar design to most large guns. Also, the overall barrel length is slightly over 56 calibers, which is "longer" than most larger guns; a replica barrel can be achieved simply by cutting off the 40mm barrel to the proper length.

A schematic of the apparatus is shown in Figure 2. Figure 3 is a photograph of the facility. The 40mm gun is mounted on a carriage which consists of two 1-in. (25.4mm) thick steel plates on which the gun is mounted, and which are connected to the bushing housings. The gun and carriage are free to move as a unit in the axial direction by means of four recirculating-ball linear bushings. Each of the two bushing housings contains two of the ball linear bushings. The bushings run on two 4-in. (101.6mm) diameter, 5-ft (1.52m) long precision steel shafts and provide very small frictional drag. The drag force for constant velocity of the gun carriage has been measured and found to be about 11 lb (5 kg). The total weight of the recoiling mass (gun and carriage) is about 600 lb (272 kg), so the coefficient of friction is about 0.018. Assuming there are no moments on the gun, the impulse of the friction force during the in-bore and gas-ejection period amounts to less than 0.3% of the total recoil impulse. The shafts are arranged one above the other to allow easy access to the gun and to provide a narrow apparatus (maximum width 10 in. or 25.4 cm), which results in a minimum of interference with the blast field. The shafts and the gun barrel were leveled to within 0.001 in. per ft (0.08mm per meter) so that gravitational effects could be ignored. The entire apparatus is structurally very rigid. A dashpot decelerates the recoiling mass. The free-recoil distance is 7 in. (178mm) before the carriage contacts the dashpot, which is sufficient for all events of interest to occur.

The recoiling mass was "balanced" so that the center of mass was located near the centerline of the gun bore, to minimize recoil moments. Such recoil moments can be very large. For example, the peak chamber pressure in the current experiment was on the order of 35,000 psi, and the bore area was about two square inches, which results in a peak recoil force of about 70,000 lbf, exerted along the bore centerline. If the center of mass were located 1/4 in. from the bore centerline, a peak recoil moment of about 1500 ft-lb would occur, resulting in a contribution to the bearing load of about 600 lb. If the center of mass were located exactly on the bore centerline, this moment would be zero. The apparatus was balanced so that the center of mass was within 1/4 in. of the bore centerline.

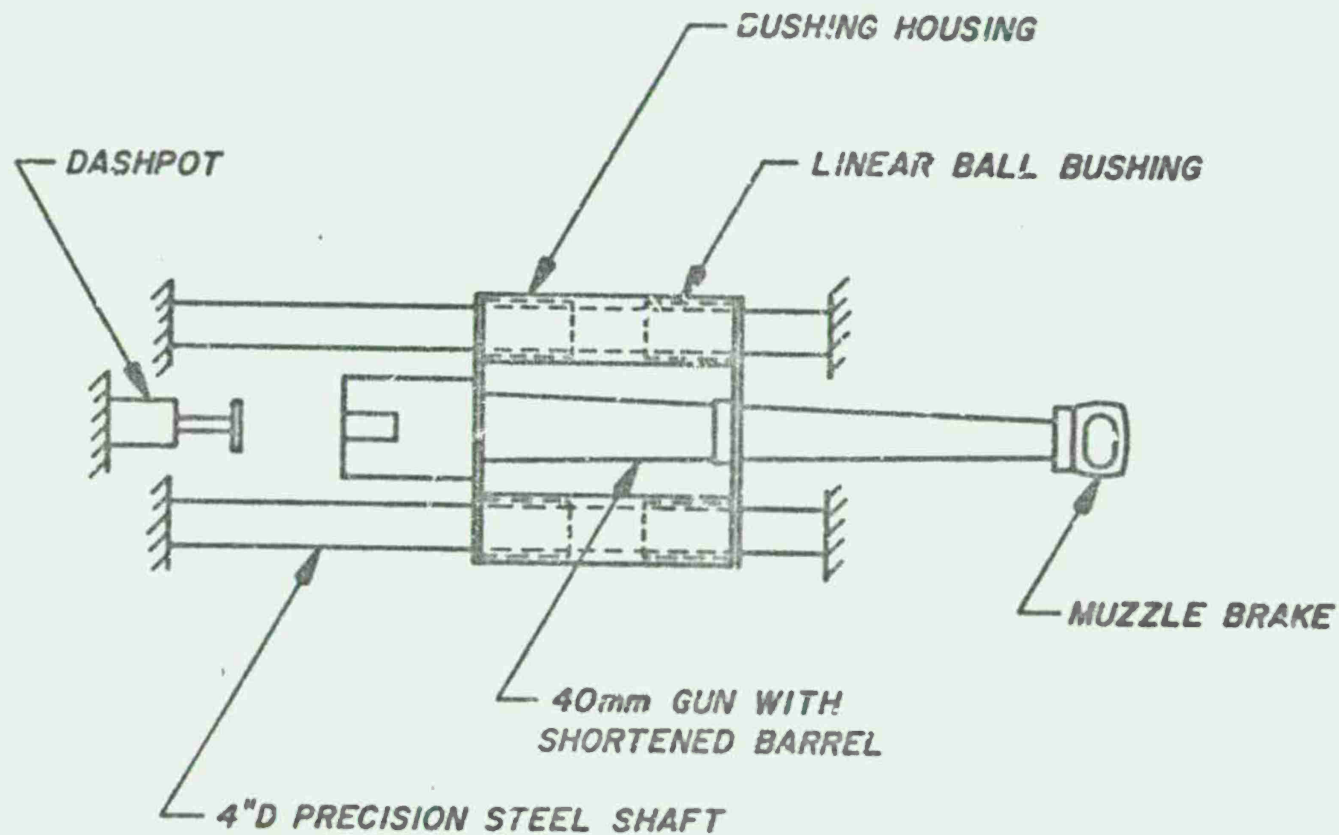


Figure 2. Schematic of 40mm Free-Recoil Gun Mount
(Side View, Scale 1/15 Actual Size)

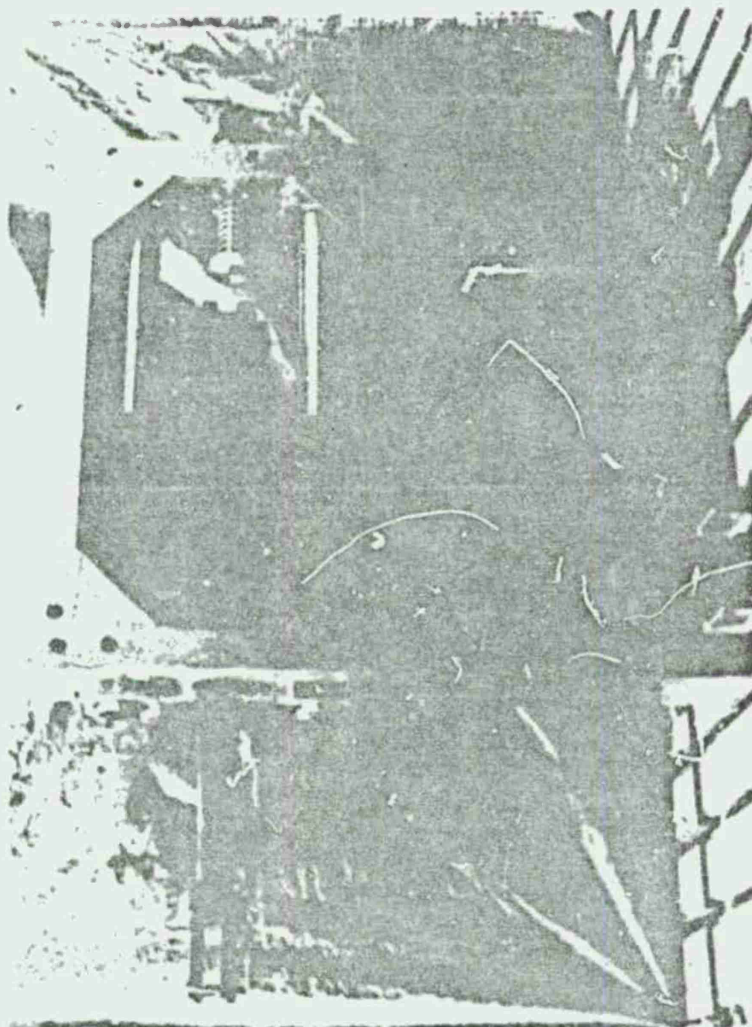


Figure 3. 40mm Free-Recoil Gun Mount

Additional bearing loads are due to the weight of the recoiling mass (600 lb) and rifling torque reaction. The rifling torque reaction was estimated to be about 400 ft-lb maximum, an equivalent bearing load of less than 100 lb. The bearings are rated for 5000 lb.

The round configuration used for the experiment is shown schematically in Figure 4. The projectile is a 40mm MK 2, modified by shortening the tapered base 0.5 in. to reduce the weight of the projectile. The modified projectiles were inert loaded to the desired weight. The 40mm MK 3 steel case was used. To reduce the chamber volume to the desired value, the case was partly filled with Stonhard Company "stonfil," a material similar to concrete. The propellant was ignited by a 20mm electric primer cap, M52A3B1, boosted by one gram of FFFFg black powder in a small silk bag. The primer cap was mounted in a special socket made of a BNC female electrical connector.

INSTRUMENTATION

The instrumentation included a timing signal, projectile velocity, muzzle pressure, and blast gages at various locations around the gun. The displacement and acceleration of the recoiling mass were also recorded. The displacement and elapsed-time records were used to obtain the velocity of the recoiling mass. These data are sufficient to determine muzzle brake effectiveness and blast field parameters.

All raw data were recorded on a Sangamo Sabre III 14-channel tape recorder, with 80 KHz (IRIG wideband Group I) record boards. A schematic of the instrumentation system is shown in Figure 5.

Two accelerometers were used, both located on the recoiling mass. The accelerometers were Bell and Howell 4-202-0001 (± 250 g) linear accelerometers. The signal from each accelerometer was fed into an Endevco 4470 signal conditioner with a 4471.1A voltage-regulated bridge conditioner, then into a Newport Model 60 dc amplifier, and finally into the tape recorder.

Muzzle pressure was recorded by means of a Kistler 607 pressure gage located in the gun tube 0.5 calibers from the muzzle. The signal was fed to a Kistler 503D6 charge amplifier, then to a Newport Model 60 dc amplifier, and then into the recorder.

Two types of blast pressure gages were used, located at various positions around the gun. The blast gages used were Crystal Research free-air pressure tourmaline ("lollipop") gages and an Atlantic Research (Celeasco LC-33) pencil gage. Each signal was fed into an Endevco Model 4470 signal conditioner with a 4477.1 charge amplifier, then into a Newport Model 60 dc amplifier, and then into the recorder.

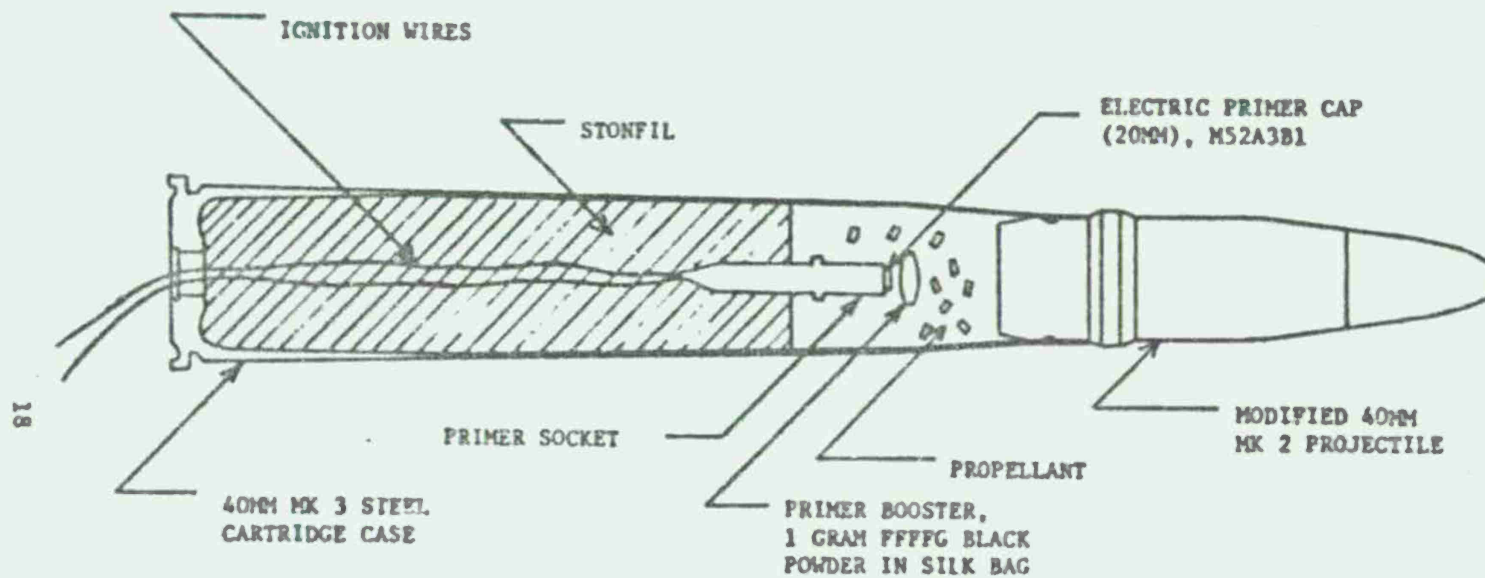


Figure 4. Round Configuration, 40mm Scaling
of 105mm

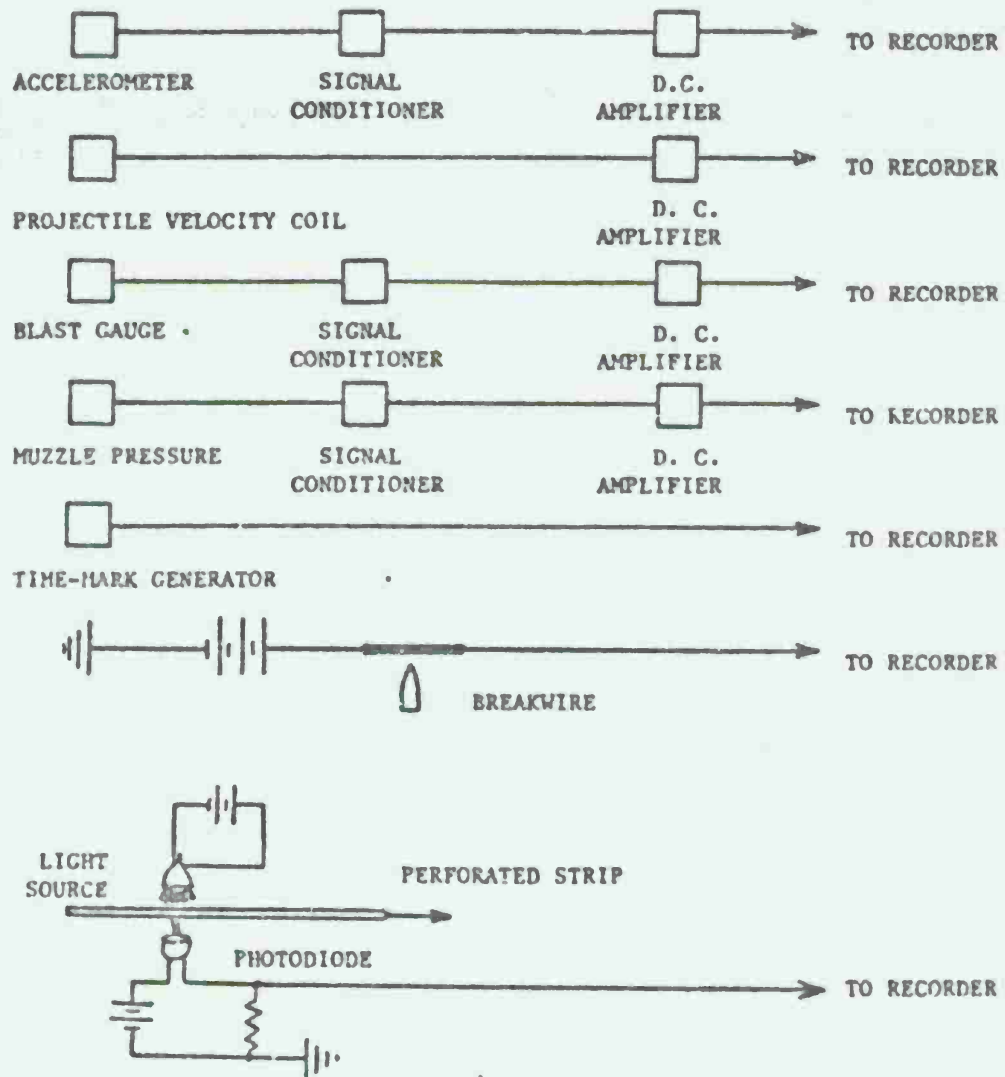


Figure 5. Instrumentation Schematic

The timing signal was generated by a Tektronix Type 184 Time-Mark Generator, fed directly into the recorder. Timing marks at 0.1, 1, and 10 ms were used.

The projectile velocity was measured by means of two, 200-turn wire-wound coils whose locations along the line of fire were accurately known. The coil locations were nominally 25 ft and 75 ft from the muzzle. The signals generated when the magnetized projectile passed through a coil were used in conjunction with the timing marks to determine the mean projectile velocity between 25 ft and 75 ft from the muzzle.

The displacement of the recoiling mass was measured by means of a photodiode and perforated strip. The perforated strip was a stainless-steel tape with .030-in. wide slots at intervals of 0.1 in. and moved with the recoiling mass. A stationary light source and photodiode were located on opposite sides of the perforated strip and viewed it through small diameter aligned holes. The photodiode was connected in series with a battery and resistor. The change in resistance of the photodiode caused a change in the voltage drop across the resistor. Thus, an electrical pulse was generated for every 0.1 in. of displacement of the recoiling mass.

EXPERIMENTAL PROCEDURES

The most important procedures for this experiment are those procedures required to achieve scaled gun performance. The major problem area in achieving the required scaled gun performance is accurately scaling the interior ballistics.

Table 4 shows parameter values which were directly controlled in the present experiment. The values shown in Table 4 are values for the prototype (105mm) gun, the ideal or desired values for the model (40mm) gun according to the model law, and the values actually used for the model gun. Response parameters, such as blast wave peak overpressure and muzzle brake effectiveness, are not listed in Table 4; they will be examined in detail later in this report.

The scaling analysis and resultant model law discussed earlier indicate that scaled performance can be achieved. In actual practice, exact scaled performance will not usually be achieved because it is not usually practical to scale all of the independent variables exactly. In the present experiment (Table 4), the greatest departure from exact scaling was the propellant. The Army 105mm Howitzer is particularly difficult to scale in this respect because it uses two different propellant grains in the charge. The gun was chosen as the prototype gun because it is the only gun for which suitable muzzle brake performance data were available. No available propellant grains

Table 4. Scaled Parameter Values

Quantity	Prototype Value	Ideal Scaled Value	Actual Model Gun Value
Caliber, c	105mm	40mm	40mm
In-bore shot travel, l	110 in.	41.9 in.	43.25 in.
Bore area, A	13.65 in. ²	1.98 in. ²	2.02 in. ²
Mass of projectile, m _p	33 lb	1.824 lb	1.824 lb
Type of propellant	M1	M1	M1
Specific impetus, RT ₀	10.13X10 ⁶ $\frac{\text{ft}^2}{\text{sec}^2}$	10.13X10 ⁶ $\frac{\text{ft}^2}{\text{sec}^2}$	10.13X10 ⁶ $\frac{\text{ft}^2}{\text{sec}^2}$
Mass of propellant, m _c	2.828 lb	0.156 lb	0.184 lb
Grain geometry	0.624 lb of SP, .014-in. web, 2.204 lb of MP, .026-in. web. (M67 charge, Zone 7)	0.034 lb of SP, .005-in. web, 0.122 lb of MP .010-in. web.	SP .014 in. web (smaller of two grains used in the standard 105mm M67 Zone 7 round). Also 1 gram FFFFG black powder primer booster.
Chamber volume, U _c	153 in. ³	8.46 in. ³	8.13 in. ³
Projectile velocity, V _p	1620 fps	1620 fps	1597 fps average

were found which were scale replicas of the prototype propellant grains. Lack of time and funds prevented having special scale replica propellant grains manufactured. Interior ballistics computer calculations indicated that, under these limitations, the best approximation of scaled performance could be obtained by simply using the smaller of the two prototype propellant grains as the model propellant, with the chamber volume, in-bore shot travel (barrel length), and mass of propellant adjusted to yield the desired muzzle velocity and pressure.

On the basis of interior ballistic calculations, three trial round configurations were selected and tested. All parameter values were as shown in Table 4 except mass of propellant, m_c , and chamber volume, U_c ; these values, and the resulting projectile velocities, are shown in Table 5. On the basis of these results, the final values shown in Figure 4 were selected.

Table 5. Scaled Charge Determination Test
(Test Data: 1 May 1973)

Number of Test Rounds Fired	m_c (lb)	U_c (in. ³)	V_p (fps)
1	.150	6.78	1420
3	.172	7.45	1556 \pm 8*
2	.183	8.13	1616 \pm 3*

*Total Variation

Initial firings resulted in misfires. The problem was found to be absorption of moisture from the stonfil by the propellant. To minimize this effect, all future rounds were loaded with propellant and assembled immediately before each test.

The experimental procedures used during testing were simple. Before beginning the test, all instrumentation was checked out and calibrated, and the rounds were assembled. The muzzle brake configuration to be tested was installed, and a round was loaded into the gun and fired.

DATA REDUCTION PROCEDURES

Raw data obtained during the test consisted of pressure for each of three blast gages, acceleration of the recoiling mass (two accelerometers), muzzle pressure, breakwire, pulses obtained from the magnetized projectile passing through the velocity coils, a pulse for each 0.1 in. of recoiling mass displacement, and elapsed time. All data were recorded on magnetic tape at 120 ips, and later played back onto a strip chart recorder. Typical raw data are shown in Figure 6 at a 1:1 playback ratio. The data records used for actual data reduction were expanded by replaying the tape at 7-1/2 ips, with a strip chart recorder speed of 120 ips (playback ratio 16:1), so that 1 ms = 2 in. on paper. Data reduction procedures are described in detail below. Sample calculations for the data shown in Figure 6 are included.

The only information extracted from the blast pressure records was the peak overpressure. The value read from the record was corrected for pressure gage "finite size" rise time effects using the method of reference (4). The location of each blast gage relative to the gun muzzle and line of fire was also known. Values of blast wave duration and time of arrival were not measured since these data were not available for the prototype (105mm) gun and muzzle brakes.

The accelerometer data are thought to be valid, but were not reduced quantitatively for reasons discussed later in this report.

Examination of a typical muzzle pressure data trace (Figure 6) shows a large-amplitude, short-duration spike followed by a pressure relaxation curve. The spike is believed to be due to the passage of the rotating band past the pressure gage, plus possibly some strip chart recorder overshoot. The value used for muzzle pressure at ejection was obtained by reading the value at the beginning of the pressure relaxation curve.

The projectile velocity was determined by measuring the elapsed time between the zero crossings of the two velocity coil signatures. For the test round shown in Figure 6, $t = 30.94$ ms. Using the known distance between the two coils (50 ft), the projectile velocity can be calculated as 1616 fps. It should be noted that this value is not actually the projectile muzzle velocity. Rather, it is the mean projectile velocity in the region between the two velocity coils, in this case between 25 ft and 75 ft from the muzzle. The response of a projectile during the time period immediately after ejection, including any velocity change, is a topic of current research interest.

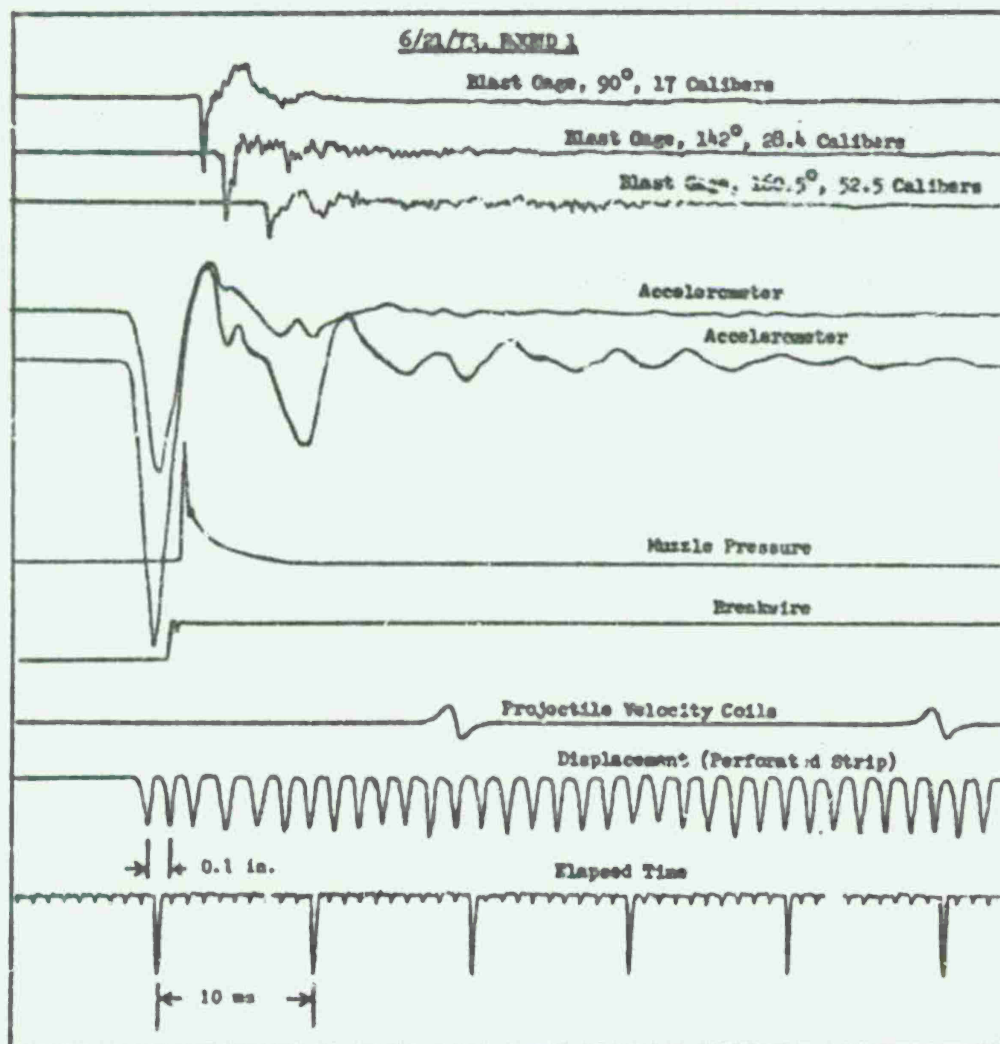


Figure 6. Typical Raw Data Record

Curves of free-recoil velocity and displacement of the recoiling mass for a realistic acceleration history are shown in Figure 7. With the present perforated strip instrumentation technique, only the terminal recoil velocity, after the end of the gas ejection period, could be determined with adequate accuracy. For the data shown in Figure 6, well after the end of gas ejection period, 40 pulses occurred in 64.53 ms, yielding a terminal recoil velocity of 5.166 fps. These pulses occurred between 2 and 6 in. of displacement.

The value of muzzle brake effectiveness may now be calculated. The definition of muzzle brake effectiveness is:

$$\beta = \frac{I_B}{G}, \quad (5)$$

where:

I_B = forward impulse due to muzzle brake;

G = gas-ejection impulse.

The value of I_B is the difference in recoiling mass final momentum for shots with and without a muzzle brake, i.e.,

$$I_B = m_{r2} V_{r2} - m_{r1} V_{r1}, \quad (6)$$

where:

m_{r2} = recoiling mass without muzzle brake;

m_{r1} = recoiling mass with muzzle brake;

V_{r2} = terminal recoil velocity without muzzle brake;

V_{r1} = terminal recoil velocity with muzzle brake.

The value of the gas-ejection impulse G is more difficult to determine. A satisfactory method would be to measure the value of recoil velocity at the instant of shot ejection. This value could be used to determine the momentum of the recoiling mass at the instant of shot ejection, which (neglecting friction) is equal to the in-bore impulse. With the in-bore impulse and total recoil impulse known, the gas-ejection impulse would easily be calculated using equation (6). However, it was not possible to measure recoil velocity at the instant of shot ejection with the present instrumentation. Thus, two alternate methods of determining G were used.

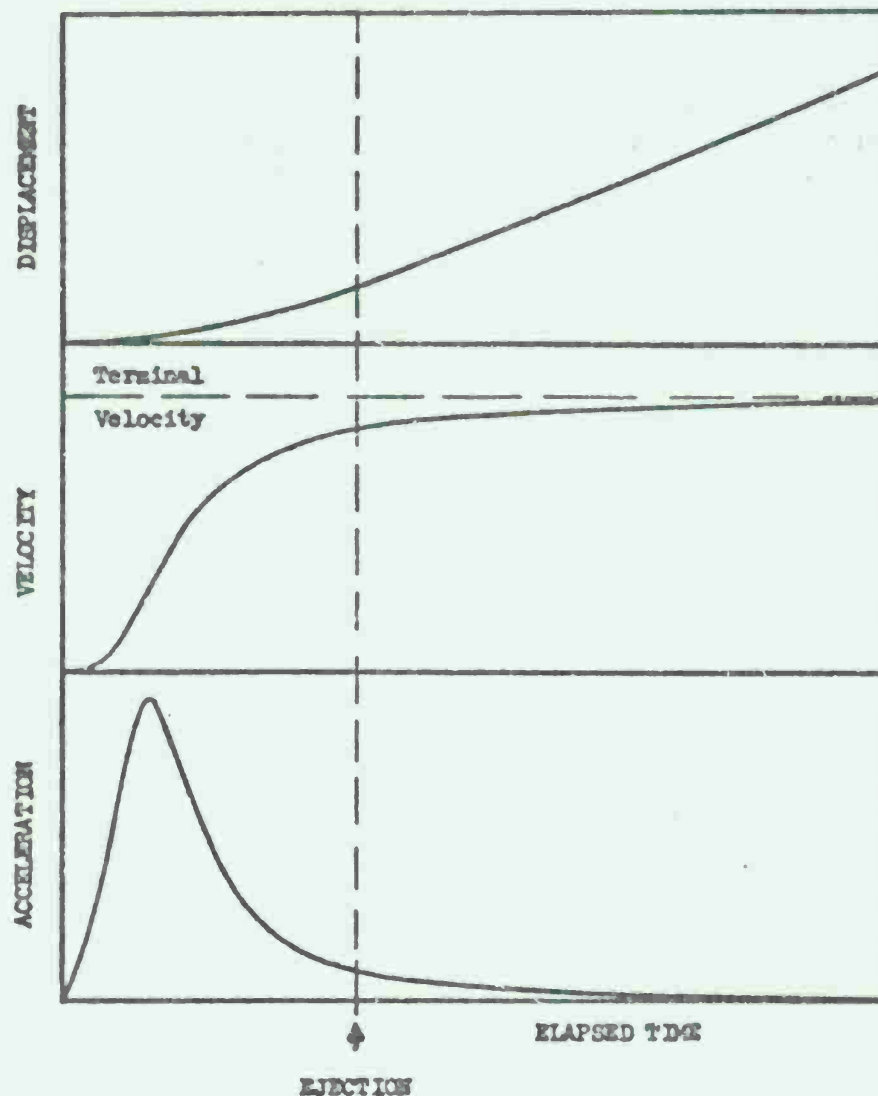


Figure 7. Representative Displacement, Velocity, and Acceleration of Recoiling Mass in Free Recoil

Of the two methods used to determine a value for G, one is experimental and one is theoretical. The experimental method relies on assuming the in-bore impulse is given by:

$$M = (m_p + \frac{m_c}{2})V_p. \quad (7)$$

Here m_p is the projectile mass and m_c is the propellant mass. The formula assumes, as is commonly done in interior ballistics, that the propellant gas velocity is linearly distributed from zero at breech to the projectile velocity at the muzzle, and that there is uniform density throughout the burned propellant. The total recoil impulse is simply the product of the recoiling mass and the terminal recoil velocity. Thus (neglecting friction),

$$G = I - M = m_{r2}V_{r2} - (m_p + \frac{m_c}{2})V_p. \quad (8)$$

The projectile velocity V_p showed significant round-to-round variation for the scaled round configuration used. The terminal recoil velocity varies directly with the projectile velocity V_p . Sufficient data were available to obtain a plot of the recoil velocity V_{r2} (without a muzzle brake) as a function of V_p . For each muzzle brake test round, the value used for V_{r2} was that which corresponded with the value of V_p for that test round.

The theoretical method (5) is:

$$G = m_c (1 + \frac{m_c}{12m_p}) (\frac{1342}{g}) \sqrt{\frac{RT_o}{10^6} - .0433 + .1486 \frac{m_p}{m_c} (\frac{V_p}{1000})^2} \quad (9)$$

This value for the 105mm prototype gun is 277 lbf-sec, which yields a 40mm scaled value of 15.3 lbf-sec. A value of β was calculated by each method for each muzzle brake test round.

RESULTS AND DISCUSSION

SCALING FEASIBILITY

One of the two objectives of the present work was to demonstrate the feasibility for reduced scale testing of muzzle devices. Selected portions of Salisbury's 105mm muzzle brake experiment were repeated at reduced scale using the 40mm free-recoil apparatus. Comparisons of

muzzle brake effectiveness data for the full-size (105mm) and reduced-scale (40mm) tests are shown in tabular form in Table 6 and in graphical form in Figure 8. The complete set of experimental data is presented in Appendix A. Worst-case experimental uncertainty for the present test (40mm) was estimated by means of logarithmic differentiation uncertainty analysis (Appendix B) and was found to be $\pm 17\%$. This is significantly smaller than had been previously attained. It is unlikely that worst case would actually occur. Maximum total variation in effectiveness values for a given brake configuration was approximately 4% in the present experiment. The values shown in Table 6 and Figure 8 are average values obtained for three test rounds for each brake configuration. The uncertainty of the 105mm data is unknown, but is thought to be significantly larger than $\pm 17\%$ (10). The variation of effectiveness values for a given brake configuration is also unknown for the 105mm data.

Table 6. Comparison of Muzzle Brake Effectiveness Data

Muzzle Brake Configuration		Muzzle Brake Effectiveness, β		
Disk Diameter (Calibers)	Distance From Muzzle (Calibers)	105mm (Salisbury)	40mm,	40mm Using
			Using Approx. Experimental Value of G	Theoretical Value of G
3.63	0.73	0.70	0.86	0.77
3.63	2.18	0.93	1.06	0.94
3.63	3.63	0.70	0.74	0.66
6.05	0.73	0.78	0.84	0.75
6.05	2.18	1.17	1.39	1.24
6.05	3.63	0.97	1.16	1.04

The maximum disagreement between 40mm and 105mm effectiveness values was 22%, while the average absolute value disagreement was 10%. These are well within the limits of experimental accuracy. The 105mm data was reduced using a theoretical value of G calculated using equation (9). A comparison of the 105mm data with the 40mm data reduced using the theoretical value of G showed a maximum disagreement of 10% and an average absolute value disagreement of 6%. In light of the large experimental uncertainty, difficulty of scaling the 105mm Howitzer, and the preliminary nature of the work, the agreement is considered to be good. With planned improvements in instrumentation and experimental

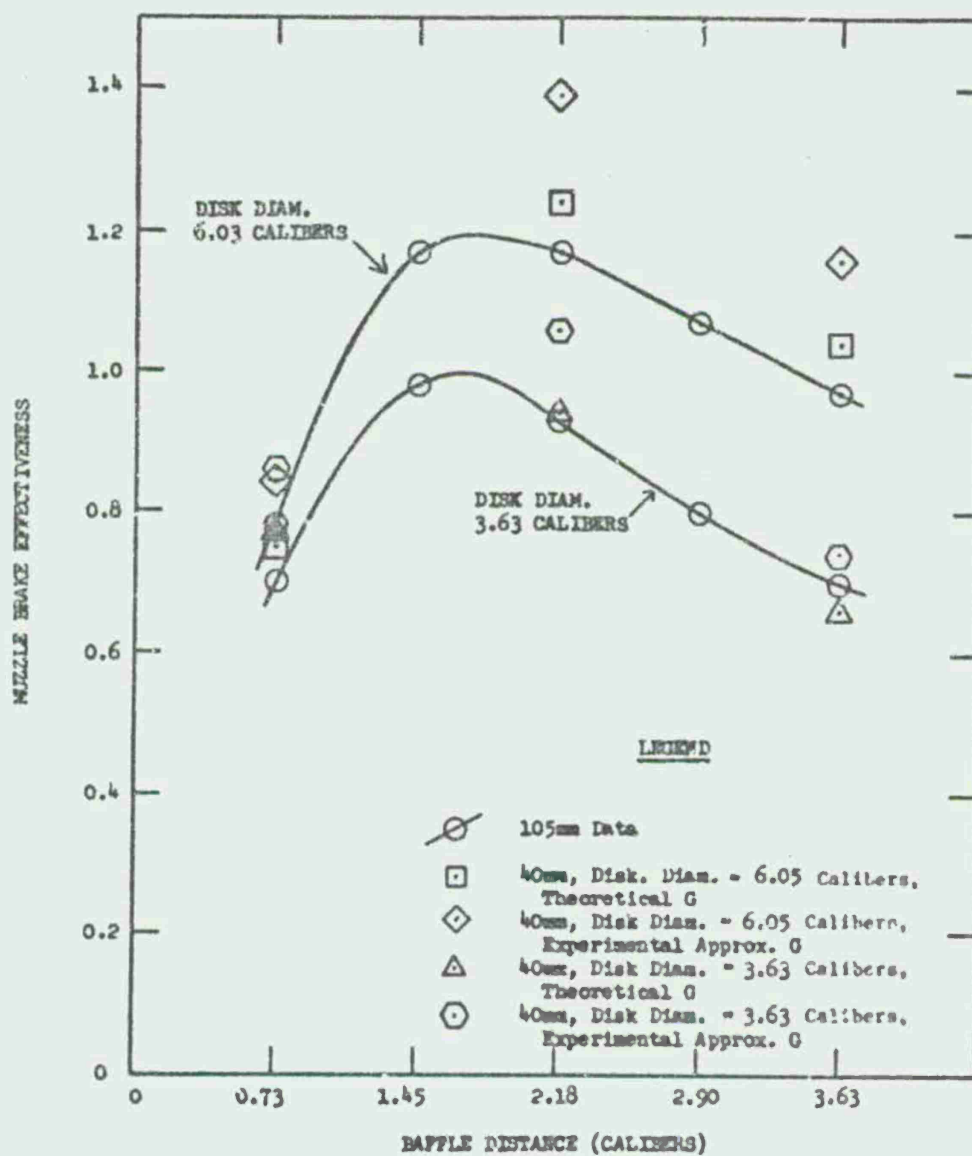


Figure 8. Comparison of Muzzle Brake Effectiveness Data

procedures, which are discussed later in this report, and for prototype guns less difficult to scale, significantly better results are expected. The conclusion is that muzzle brake effectiveness can be successfully studied at reduced scale.

The second response parameter of primary interest in this reduced scale investigation was blast overpressure in the region behind the muzzle. Scaling of blast overpressures has been achieved in the past (7,8). Successful scaling of blast field with a conical muzzle device was reported in reference (9). Also, some blast data obtained in the present experiment (Table A-2) can be compared with available 105mm blast data taken at NWL (10). Detailed blast data obtained during the test reported in (10) are shown in Table 7. Comparison of average blast overpressures for the 105mm and 40mm without brakes is shown in Table 8. The agreement is excellent. This result is especially important because the gages are located in a region behind the muzzle, in the crew area, which is the region of most interest for muzzle brake investigation. Thus, there is sufficient information to conclude that blast overpressures can be successfully studied at reduced scale.

Table 7. 105mm Blast Data

Test Data: 16-18 March 1973

Test Description: 105mm Howitzer, M67 Zone 7 Charge, No Diffuser -
Blast pressures measured at various locations around the gun.

Round No.	Charge Temperature (°F)	Blast Pressure (psi) @ Location	
		135°, 20.3 Calibers	165°, 20.3 Calibers
24	90	1.2	0.9
25	90	1.3	1.0
26	90	1.2	0.9
27	90	1.3	1.1
28	90	1.2	0.9
29	0	1.2	1.2
30	0	1.2	1.1
31	0	1.2	1.1
32	0	1.2	1.2
33	0	1.2	1.1

Table 8. Comparison of Blast Overpressure Results Without Muzzle Brake

Gun, Charge Temperature (°F)	Blast Pressure (psi) @ Location	
	135°, 20.3 Calibers	165°, 20.3 Calibers
105mm, 90°F	1.2	1.0
105mm, 0°F	1.2	1.1
40mm, = 70°F	1.2	1.1

The blast overpressure data with muzzle brakes present did not show good agreement between the full-size (105mm) and reduced-scale (40mm) test results. Comparison of results from Tables A-5 and A-6 and from reference (3) is shown in Figure 9. All data points are average values of several rounds. The most obvious discrepancy is that the 105mm blast data are considerably higher than the reduced scale (40mm) data. There is a possibility that the 105mm blast gage location reported (3) is incorrect and that the gage was in fact much closer to the muzzle (6). If this were the case, the discrepancy would be explained. Other possible sources of disagreement are as follows. The reduced-scale 40mm gun utilized a muzzle collar that, for construction reasons, was larger than an exact scale model of the collar used on the full-size 105mm gun. This "larger" collar had no apparent effect on the effectiveness of the muzzle brake, but may have provided some shielding from blast effects. Also, the blast gages used in the present 40mm test were not completely satisfactory for measurement of small caliber blast. The validity of the 105mm blast data is unknown; these data were obtained by methods which, by today's standards, are quite unsophisticated. Thus, while no conclusions are drawn from these data, the results discussed in the previous paragraph are sufficient to conclude that blast overpressure can be successfully studied at reduced scale.

DEVELOPMENT OF APPARATUS AND PROCEDURES

The second objective was to develop apparatus and procedures for use in future reduced-scale investigations of muzzle devices. Important aspects include the free-recoil gun mount, scale round configurations, and procedures for accurately scaling and measuring the performance parameters of interest.

The free-recoil 40mm gun mount apparatus is quite satisfactory. In particular, the concept of using shafts and linear ball bushings to carry the gun was found to be highly satisfactory. This arrangement offers less friction, more positive guidance, greatly simplified construction, and less maintenance than the wheels and tracks system used for previous free-recoil gun mounts.

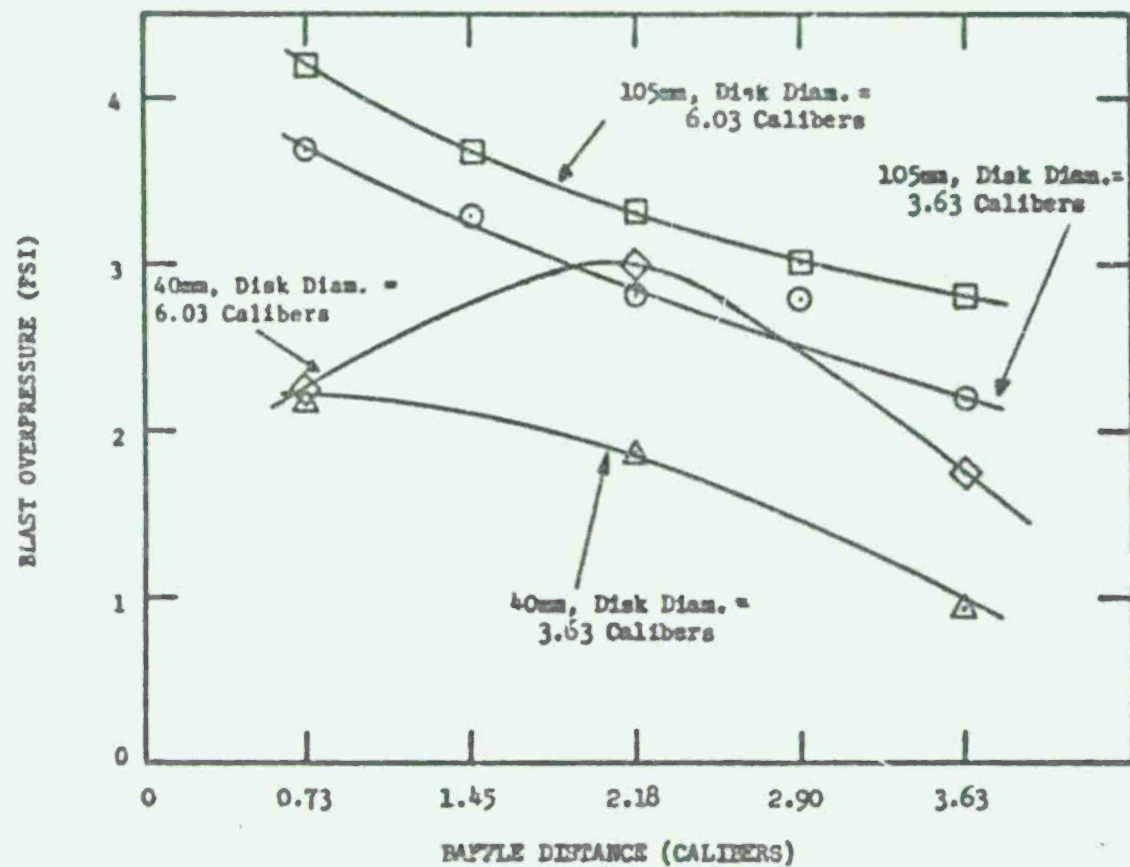


Figure 9. Comparison of Blast Overpressure With Muzzle Brake; Gage Location 142°, 28.4 Calibers

The round configuration used was not completely satisfactory. The biggest problem was fairly large round-to-round variations; for example, projectile velocity varied from 1568 to 1619 ft/sec, with an average of 1597 ft/sec for 32 rounds. The most probable reason for these variations was variations in the chamber volume, a result of using Stonfil to reduce the chamber volume. The level of the Stonfil was difficult to control closely. Also, the Stonfil was permanently deformed during firing, as evidenced by a drop in the Stonfil level. However, the amount of deformation was not consistent. Moisture from the Stonfil was also a problem. For future tests, cartridge case volume will be reduced, when necessary, by means of metal slugs.

Other round configuration problems were the primer and the propellant. The small electric primer cap will be replaced by a standard 40mm percussion cap with an extended flash tube. The propellant used was not a true scale replica of the prototype propellant. In tests in which very accurate scaling is required, special scaled propellant grains could be manufactured.

It was originally planned to directly measure recoil force as a function of time. Such information would be valuable to the gun designer, especially during design of recoil systems. The technique used was accelerometers on the recoiling mass to measure the acceleration as a function of time; with the gun in free recoil and the mass known, the recoil force as a function of time could easily be calculated. The accelerometer record was expected to look like the curve shown in Figure 7. Instead, it showed large oscillations, as shown in Figure 6.

The reason for this behavior is as follows. Recall that the gun carriage is essentially composed of a gun located between two bushing housings, connected by yoke plates (Figure 2). When the gun is fired, it begins to move. The massive bushing housings at first lag behind the gun. Then the yoke plates, acting like springs, accelerate the bushing housings until they actually pass the gun. The plates then accelerate the gun past the bushing housings, and so on. The result is a more or less sinusoidal vibratory motion superimposed on the rigid body motion due to the recoil forces. To investigate this motion, a computerized vibration analysis was carried out by Mr. T. F. Morris of NWL. In this analysis, the gun carriage was modeled as a system of springs and masses. The results indicated that the relative displacements of the gun and bushing housings relative to the center of mass of the recoiling mass were very small, on the order of 0.001 in. This was expected, since the gun carriage was designed to be structurally very rigid. However, the accelerations of the gun and bushing housings relative to the center of mass were as large as ± 50 g, while the maximum acceleration of the center of mass was 127 g. The analytical acceleration history agreed quite well with the experimental results.

Changes made in parameter values in the analysis indicated that the problem was not feasible to solve by increasing the stiffness. Thus, the acceleration of the recoiling mass will not be used to determine the recoil force-time history. The recoil force-time history could be obtained from other data, such as recoil velocity-time history, but the accuracy might be questionable. Even approximate recoil force data would, however, be of use to the gun designer.

The greatest drawback of the procedures used in the current test was lack of an accurate experimental determination of the gas-ejection impulse, G . A desirable method of accurately determining G would be to accurately measure the recoil velocity at the instant of projectile ejection, as well as the terminal free-recoil velocity. Then one could use, with or without a muzzle brake,

$$G = m_r(V_{rt} - V_{rp}), \quad (10)$$

where:

V_{rt} = terminal recoil velocity;

V_{rp} = recoil velocity at the instant of projectile ejection.

The required accuracy is extreme. A logarithmic differentiation uncertainty analysis shows that for a recoil velocity on the order of 5 ft/sec, the gas ejection impulse G could be determined within $\pm 5\%$ if the recoil velocities could be determined with an uncertainty of ± 0.02 ft/sec ($\pm 0.4\%$). The terminal recoil velocity was measured in this experiment with an uncertainty of $\pm 0.16\%$ (Appendix B). The recoil velocity at the instant of projectile ejection is much more difficult to measure, primarily because the recoil velocity is changing rapidly (Figure 7). Very fine resolution of both time and displacement are required. Very accurate measurement of elapsed time offers no difficulty. Hence, the problem comes down to accurately measuring the displacement of the recoiling mass. A promising possibility is a commercially available device known as a "linear encoder." This device uses a very fine, accurately-scribed grid on a glass strip, along with a phototransistor, light source, and electronic circuitry, to emit an electrical pulse for every 0.0005 in. of displacement. It appears that this device could be successfully used to measure the recoiling mass displacement with sufficient accuracy. A very accurate determination of the instant of projectile ejection will also be required. This will probably be achieved by a breakwire located such that the circuit is broken just as the base of the projectile passes through the muzzle plane. Finally, an efficient data reduction procedure would be required to utilize such detailed data.

In conclusion, the apparatus and procedures developed during this test, with minor modifications, are suitable for reduced-scale testing of muzzle devices.

SUMMARY OF CONCLUSIONS

Comparison of results of the present experiment with previous results of other experimenters has resulted in good agreement for values of muzzle brake effectiveness and blast overpressures. In addition, good results for scaling of blast overpressure had previously been obtained. Thus, sufficient data are available to conclude that muzzle devices can be accurately investigated and developed at reduced scale, with considerable savings of time and money.

The experimental apparatus and procedures necessary for reduced scale muzzle brake testing were developed during this test. The apparatus and procedures that have been developed are, with minor modifications, satisfactory for carrying out reduced-scale testing of muzzle devices.

REFERENCES

1. Maillie, F. H., *Finite Difference Calculations of the Free-air Blast Field About the Muzzle and a Simple Muzzle Brake of a 105mm Howitzer*, NWL Technical Report TR-2938, Naval Weapons Laboratory, Dahlgren, Virginia, April 1973.
2. East, J., *Scaling of Interior Ballistics*, Unpublished Analysis, Naval Weapons Laboratory, Dahlgren, Virginia, December 1972.
3. Salisbury, M. J., *The Effects of a Muzzle Brake's Diameter and Length on Overpressure and Efficiency*, Technical Report 66-2920, Rock Island Arsenal, Rock Island, Illinois, October 1966.
4. Moore, G. R., *Response of a Finite Circular Crystal Transducer Element to a Friedlander Pressure Pulse*, NWL Technical Note TN-T-12/72, Naval Weapons Laboratory, Dahlgren, Virginia, June 1972.
5. Nerdahl, M. C., *Approximate Determination of Breech Force as a Function of Time*, Technical Note A6-71, Rock Island Arsenal, Rock Island, Illinois, November 1971.
6. Private communication between M. J. Salisbury, Rock Island Arsenal, and L. L. Pater, Naval Weapons Laboratory.
7. SooHoo, G. and G. R. Moore, *Scaling of Naval Gun Blast Peak Overpressures*, NWL Technical Note TN-T-7/72, Naval Weapons Laboratory, Dahlgren, Virginia, August 1972.
8. Westine, P. S., *Modeling the Blast Field Around Naval Guns and Conceptual Design of a Model Gun Blast Facility*, Final Technical Report 02-2643-01, Southwest Research Institute, San Antonio, Texas, September 1970.
9. SooHoo, G. and J. J. Yaglia, *Use of a Conical Muzzle Device to Control Gun Blast*, NWL Technical Report TR-2793, Naval Weapons Laboratory, Dahlgren, Virginia, August 1972.
10. Marino, C. J., *Polar Blast Fields About 105mm Cannon; 105mm Cannon with Diffuser, and 40mm Cannon as Applied to the C-130 Gunship*, NWL Technical Note TN/G-36/71, Naval Weapons Laboratory, Dahlgren, Virginia, June 1971.

Table A-1. Masses of Apparatus

<u>Recoiling Mass</u>	<u>Weight (lb)</u>
Without muzzle brake	601
With large disk	612
With small disk	607

$$(m_p + \frac{m_c}{2}) = 1.916 \text{ lb}$$

where:

$$m_p = 1.824 \text{ lb}$$

$$m_c = 0.164 \text{ lb}$$

Table A-2. Experimental Data

Test Date: 1 May 1973

Test Description: Charge Determination Test - Last two rounds provide data for comparison with NWL 103mm blast data. No muzzle device present. Charge temperature approximately 70°.

Round No.	m_c (grams)	v_p (ft./sec)	Blast Pressure (psi) @ Location (type of gage)		
			90°, 20.3 Calibers (lollipop)	135°, 20.3 Calibers (lollipop)	165°, 20.3 Calibers (lollipop)
1	68	1420	3.61	1.27	1.02
2	78	1548	3.99	1.27	1.02
3	78	1562	3.53	1.24	1.06
4	78	1558	3.68	1.27	1.31
5	83	1619	4.17	1.26	1.06
6	83	1613	4.06	1.16	1.19

Table A-3. Experimental Data

Test Date: 24 May 1973

Test Description: No muzzle brake. Final round configuration, 83.5 gram propellant. Useful pressure data obtained. Displacement transducer malfunctioned, so valid values of terminal recoil velocity were not obtained. Temperature approximately 70°F.

Round No.	V p (fps)	Muzzle Pressure (psi)	Blast Pressure (psi) @ Location (type of gage)		
			90°, 17 Calibers (lollipop)	270°, 17 Calibers (pencil)	142°, 28.4 Calibers (lollipop)
1	1595	3300	4.58	4.76	1.00
2	1597	3300	4.66	4.76	0.98
3	1598	3300	4.46	4.48	1.00
4	1594	3400	4.62	4.72	1.03
5	1593	-	4.46	4.68	1.00
6	1620	3600	4.54	4.52	0.95

Table A-4. Experimental Data

Test Date: 7 June 1973

Test Description: No muzzle brake. Measured pressures and recoil velocity.

Round No.	v p (fps)	Muzzle Pressure (psi)	Terminal Recoil Velocity (fps)	Blast Pressure (psi) @ Location (type of gage)		
				90°, 17 Calibers (lollipop)	270°, 17 Calibers (pencil)	142°, 28.4 Calibers (lollipop)
1	1597	3000	5.858	4.91	4.65	0.91
2	1606	3000	-	4.71	4.57	0.88
3	1593	3100	5.187	4.71	4.53	0.86

Table A-5. Experimental Data

Test Date: 20 June 1973

Test Description: Muzzle brake configuration as indicated. This test is the reduced-scale muzzle brake test. Recoil velocity is average from 2-in. to 6-in. recoil distance.

Round No.	Muzzle Brake Configuration		V _p (fps)	Terminal Recoil Velocity (fps)	Muzzle Pressure (psi)	Blast Pressure (psi) @ Location (type of gage)	
	Disk Diameter (in.)	Distance from Muzzle (in.)				90°, 17 Calibers (lollipop)	142°, 28.4 Calibers (pencil)
1	-	-	1603	5.826	-	4.43	0.92
2	-	-	1606	5.847	3200	4.38	0.92
3	-	-	1584	5.800	3100	4.64	0.96
4	9.524	5.715	-	-	3300	6.08	1.72
5	↓	↓	1596	4.880	3100	6.49	1.72
6	↓	↓	1600	4.892	3200	6.23	1.85
7	↓	3.429	1600	4.727	3500	12.60	3.60
8	↓	↓	1578	4.661	3100	11.20	2.64
9	↓	↓	1597	4.714	3000	11.50	2.84
10	↓	1.143	1581	5.059	2900	9.29	2.21
11	↓	1.143	1588	5.102	2900	8.28	2.28

A-5

Table A-6. Experimental Data

Test Date: 21 June 1973

Test Description: Same as 20 June 1973

Round No.	Muzzle Brake Configuration		V _p (fps)	Terminal Recoil Velocity (fps)	Muzzle Pressure (psi)	Blast Pressure (psi) @ Location (type of gage)	
	Disk Diameter (in.)	Distance from Muzzle (in.)				90°, 17 Calibers (lollipop)	142°, 28.4 Calibers (pencil)
1	9.524	1.143	1616	5.166	3100	8.69	2.18
2	5.715	5.715	1593	5.210	2800	5.76	0.99
3	↓	↓	1595	5.232	2900	5.86	0.92
4			1594	5.222	3100	5.76	0.89
5		3.429	1596	4.961	3000	8.38	2.18
6		↓	1594	5.001	2500	8.18	1.72
7			1597	4.992	3100	8.28	1.75
8		1.143	1590	5.126	2800	6.97	2.05
9		↓	1594	5.131	3100	7.88	2.38
10			1607	5.164	3000	7.58	2.08
11	-	-	1568	5.727	3100	4.44	0.96

9-V

Table A-7. Reduced Experimental Data for
Muzzle Brake Effectiveness

Test Date	Round No.	Muzzle Brake Configuration		Muzzle Brake Effectiveness, β	
		Disk Diameter (in.)	Distance From Muzzle (in.)	Based on Experimental Approximation of G	Based on Theoretical Value of G
6/20/73	4	9.524	5.715	-	-
	5		↓	1.16	1.04
	6		↓	1.16	1.04
	7		3.429	1.39	1.25
	8		↓	1.39	1.23
	9		↓	1.40	1.25
	10		1.143	0.85	0.75
	11		↓	0.82	0.73
6/21/73	1		↓	0.85	0.77
	2	5.715	5.715	0.75	0.57
	3		↓	0.73	0.65
	4		↓	0.74	0.66
	5		3.429	1.06	0.94
	6		↓	1.06	0.93
	7		↓	1.07	0.93
	8		1.143	0.85	0.76
	9		↓	0.86	0.77
	10		↓	0.87	0.79

EXPERIMENTAL UNCERTAINTY ANALYSIS

This appendix presents estimates of the maximum uncertainty, or possible error, in experimentally measured quantities.

PRESSURE MEASUREMENTS

The errors in the pressure measurements are most difficult to assess for both the muzzle pressure and free-air blast pressure. A large part of the difficulty is because the pressure is highly transient. Sources of error include calibration inaccuracies, thermal sensitivity, overshoot, rise time, and uncertainty in the location of the gage. Another source of error in measuring peak overpressure is rise time due to the finite (i.e., not infinitesimal) size of the gage sensing element. The measurements in this experiment were corrected for this effect, according to the method described in reference (5). Errors can also appear as a result of the data recording and playback apparatus. The situation is further complicated by the fact that the actual pressure is not necessarily consistent, for example, due to round-to-round variations in the projectile and charge assembly. Examination of test records, plus past experience, indicate that the uncertainty in free-air blast pressure measurements is on the order of $\pm 10\%$. The uncertainty of the muzzle pressure measurements is estimated to be of the same order, perhaps somewhat smaller.

LOGARITHMIC DIFFERENTIATION TECHNIQUE

Because of experimental uncertainties in measured quantities, there is also uncertainty in the value of any calculated parameter that involves measured quantities. Such uncertainties are estimated in this report by means of the "logarithmic differentiation" technique.

As an example of the logarithmic differentiation technique, consider a hypothetical parameter Q , defined as:

$$Q = \frac{BW^2}{S},$$

where B , S , and W are hypothetical, experimentally-measured quantities. Taking the natural log of both sides of this equation yields:

$$\ln Q = \ln B + 2 \ln W - \ln S.$$

Differentiating both sides of this equation yields:

$$\frac{dQ}{Q} = \frac{dB}{B} + 2 \frac{dW}{W} - \frac{dS}{S}.$$

The differential quantities are taken to represent the uncertainties in each quantity. For example, dB represents the uncertainty in the measured value of B. Similarly, dQ represents the uncertainty in the calculated value of Q. The maximum uncertainty in the calculated parameter Q can be obtained by taking absolute values:

$$\left| \frac{dQ}{Q} \right| \leq \left| \frac{dB}{B} \right| + 2 \left| \frac{dW}{W} \right| + \left| \frac{dS}{S} \right|$$

This technique is applied to the present experiment in the following paragraphs.

PROJECTILE VELOCITY

The projectile velocity was measured by measuring the elapsed time for the projectile to traverse a known distance.

$$V_p = \frac{L}{t}$$

Using the logarithmic differentiation technique,

$$\frac{dV_p}{V_p} = \pm \left[\left| \frac{dL}{L} \right| + \left| \frac{dt}{t} \right| \right]$$

The velocity coils were located at 25 ft and 75 ft, so $L = 50$ ft, with an uncertainty of $dL = \pm 0.5$ in. = $\pm .042$ ft. The elapsed time was about 31 ms, with $dt = \pm 0.05$ ms. Thus, $V_p = 1612$ ft/sec, which results in an uncertainty of 0.25%, or 4 ft/sec, in the muzzle velocity. Measured values of V_p show more variation because of round-to-round variation. It is noted that this value of V_p is not the true "muzzle velocity" because of the blast wave interaction with the projectile, and drag, though it is probably different by only a few feet per second.

TERMINAL RECOIL VELOCITY

The terminal recoil velocity of the recoiling mass was determined by measuring the elapsed time required to travel a distance of 4 in. at constant velocity. Thus,

$$V_{rt} = \frac{L}{t}$$

and

$$\left| \frac{dv_{rt}}{v_{rt}} \right| \leq \left| \frac{dL}{L} \right| + \left| \frac{dt}{t} \right|.$$

The uncertainty of the travel ($L = 4$ in.) results from inaccuracies in the location of the slots in the perforated strip, which were measured to be $dL = \pm .003$ in. maximum. The minimum elapsed time was about 57 ms, with an uncertainty of $dt = \pm .05$ ms. For $v_{rt} = 5.8$ ft/sec, the uncertainty in the terminal recoil velocity is ± 0.01 ft/sec, or 0.16%.

MUZZLE BRAKE EFFECTIVENESS

The value of muzzle brake effectiveness is calculated from:

$$\beta = \frac{I_B}{G}.$$

so:

$$\frac{d\beta}{\beta} = \pm \left[\left| \frac{dI_B}{I_B} \right| + \left| \frac{dG}{G} \right| \right].$$

The impulse due to the muzzle brake was calculated from:

$$I_B = m_{r2} v_{r2} - m_{r1} v_{r1}.$$

Logarithmic differentiation yields:

$$\frac{dI_B}{I_B} = \frac{m_{r2} dv_{r2} + v_{r2} dm_{r2} - m_{r1} dv_{r1} - v_{r1} dm_{r1}}{m_{r2} v_{r2} - m_{r1} v_{r1}}.$$

or, for worst case:

$$\frac{dI_B}{I_B} = \pm \left[\frac{m_{r2} |dv_{r2}| + v_{r2} |dm_{r2}| + m_{r1} |dv_{r1}| + v_{r1} |dm_{r1}|}{m_{r2} v_{r2} - m_{r1} v_{r1}} \right]$$

Using the following values:

$$m_{r2} = 601 \text{ lb}$$

$$dm_{r2} = \pm 2 \text{ lb}$$

$$m_{r1} = 612 \text{ lb}$$

$$dm_{r1} = \pm 2 \text{ lb}$$

$$V_{r2} = 5.820 \text{ ft/sec}$$

$$dV_{r2} = .0093 \text{ ft/sec}$$

$$V_{r1} = 4.880 \text{ ft/sec}$$

$$dV_{r1} = .0078 \text{ ft/sec}$$

the result is:

$$\frac{dI_B}{I_B} = \pm 6.2\%$$

The value of G was calculated by two methods: one of which was by means of a theoretical equation; the other from experimental data. The experimental method used the equation:

$$G = m_{r2} V_{r2} - (m_p + \frac{m_c}{2}) V_p$$

Logarithmic differentiation yields:

$$\frac{dG}{G} = \left[\frac{m_{r2} \left| \frac{dV_{r2}}{V_{r2}} \right| + V_{r2} \left| \frac{dm_{r2}}{m_{r2}} \right| + (m_p + \frac{m_c}{2}) \left| \frac{dV_p}{V_p} \right| + V_p \left(\left| \frac{dm_p}{m_p} \right| + \frac{1}{2} \left| \frac{dm_c}{m_c} \right| \right)}{m_{r2} V_{r2} - (m_p + \frac{m_c}{2}) V_p} \right]$$

Using the values:

$$m_{r2} = 601 \text{ lb}$$

$$dm_{r2} = \pm 2 \text{ lb}$$

$$V_{r2} = 5.820 \text{ ft/sec}$$

$$dV_{r2} = \pm .0093 \text{ ft/sec}$$

$$m_p + \frac{m_c}{2} = 1.916 \text{ lb}$$

$$dm_p = \pm .01 \text{ lb}$$

$$V_p = 1600 \text{ ft/sec}$$

$$dm_c = \pm .4 \text{ g} = \pm .001 \text{ lb}$$

$$dV_p = \pm 4 \text{ ft/sec}$$

the result is:

$$\frac{dG}{G} = \pm 10.6\%$$

Collecting results,

$$\frac{d\delta}{\delta} = \pm 16.8\%.$$

The difficulty in accurately measuring muzzle brake effectiveness can be seen. Actually, the uncertainty may be somewhat larger, since the expression used to calculate the value of G is only a good approximation. No formal uncertainty estimates for previous muzzle brake performance data were found. It is believed that such uncertainties were of the order of $\pm 30\%$. An uncertainty in δ of $\pm 17\%$ represents a considerable improvement. Planned future improvements in instrumentation and procedures are expected to further reduce this uncertainty to about $\pm 10\%$, primarily by reducing the uncertainty in the value of gas-ejection impulse G .

UNCLASSIFIED

**PLEASE DO NOT RETURN
THIS DOCUMENT TO DTIC**

**EACH ACTIVITY IS RESPONSIBLE FOR DESTRUCTION OF THIS
DOCUMENT ACCORDING TO APPLICABLE REGULATIONS.**

UNCLASSIFIED